Int. J. Solids Structures Vol. 19, No. 1, pp. 25–31, 1983
Printed in Great Britain.

0020-7683/83/010025-07$03.00/0

THE OPTIMAL SHAPE OF AN EARTH PENETRATING PROJECTILE

DAVID Z. YANKELEVSKY

Civil Engineering Department, Technion—Israel Institute of Technology, Haifa, Israel 32000

(*Received* 12 *October* 1981; *in revised form* 17 *February* 1982)

Abstract—The optimal shape of an earth penetrating projectile is investigated. Based on the Discs-Model, earlier developed by the author, the interaction pressure is expressed as function of the nose shape. The instantaneous resistive force is minimized to yield and optimal shape function. The optimal shape is found to be dependent on a single parameter of velocity, deceleration and medium properties.

INTRODUCTION

Many studies have been devoted to projectile penetration into earth media. The common problem is to predict deceleration history, penetration depth, interaction pressure distribution and medium response when projectile and target data are known. The procedures may be gathered into the following main groups:

(1) Empirical formulae based on curve fitting to test data, which predict penetration depth[1, 2].

(2) Models based on the Spherical or the Cylindrical cavity expansion theory[3, 4]. These simplified methods do not properly represent the soil-projectile interaction and showed poor agreement when compared with test data[5].

(3) Two-dimensional wave propagation computer codes[6–8] to predict the normal penetration of a rigid or deformable projectile. These codes are based on the governing field equations and predict the most detailed information regarding medium and projectile response.

Recently a new one-dimensional analytical model has been developed[9] in which the target is represented by a set of discs, thus reducing the penetration event into a one-dimensional problem. The target material is modeled by an equivalent locked hydrostat and an equivalent constant shear pressure relation. The nonlinear relationships of the volumetric stress vs strain and the principal stress difference at failure vs volumetric stress have been transformed into the equivalent locking model by introducing new parameters of average volumetric strain and volumetric stress. These parameters correspond according with the nonlinear relationship and found by equating the internal work done by the average values over the stressed zone to that done by the variable stresses and strains. The analysis of a typical disc response yields an expression for the interaction pressure as function of the disc properties, the projectile nose shape and the instantaneous values of velocity and deceleration. Comparisons of the discs model with test data and two-dimensional code predictions, in the low and high velocity range, show very good agreement[9, 10].

Previous studies on penetration are always based on a given nose shape. Hereunder a general shape function is taken and the corresponding expression for the resistive force is developed. The optimal nose shape that yields the minimum resistive force is analyzed using variational techniques.

FORMULATION OF THE PROBLEM

Consider a projectile penetrating through a semi infinite soil medium where the axis of penetration is normal to the top surface (Fig. 1). When the discs model is adopted, the expression for the interaction pressure is (9):

$$p(Z, t) = P_{st} + A \cdot \dot{R}^2(Z, t) + B \cdot R(Z, t) \cdot \ddot{R}(Z, t) \tag{1}$$

$$p_{st} = \frac{1}{2} \tau \ln\left(\frac{1}{\epsilon}\right) \tag{1a}$$

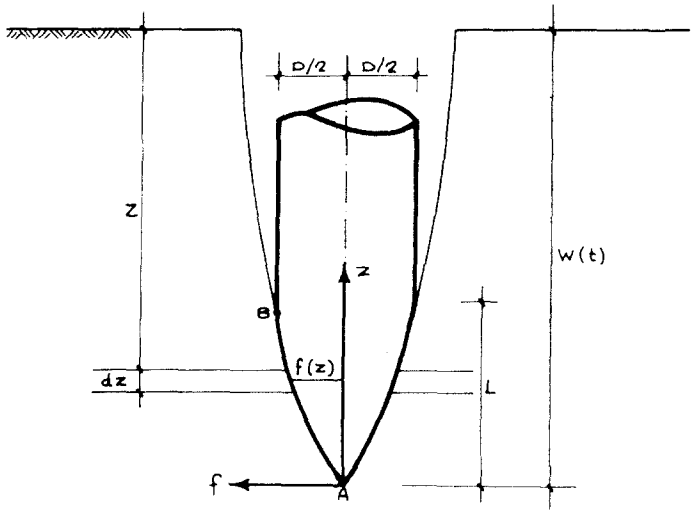

Fig. 1. Geometry for projectile and idealized medium.

$$A = \frac{1}{2}\rho_0 + \frac{1}{2}\rho \ln\left(\frac{1}{\epsilon}\right) \tag{1b}$$

$$B = \frac{1}{2}\rho \ln\left(\frac{1}{\epsilon}\right) \tag{1c}$$

where: $p(Z, t)$ = the radial component of the interaction pressure on a disc at depth Z; $R(Z, t)$, $\dot{R}(Z, t)$, $\ddot{R}(Z, t)$ = the internal boundary radial values of displacement, velocity and acceleration; τ = average principal stress difference at failure; ϵ = the average volumetric locking strain; ρ_0 = the free field mass density; and ρ = the mass density behind the plastic shock front. A local coordinate system is attached to the nose tip, and the local coordinate along the nose may be expressed as follows:

$$z = W(t) - Z \qquad 0 \leq z \leq L \tag{2}$$

where $W(t)$ is the nose tip penetration depth. The projectile nose of length L is described by the general shape function $f(z)$ which is assumed to have continuous first and second derivatives and to satisfy the boundary conditions:

$$f(0) = 0 \tag{3a}$$

$$f(L) = D/2. \tag{3b}$$

At any distance z its value is identical with the local radius $R(Z, t)$:

$$R(Z, t) = f(z). \tag{4}$$

Using the chain rule the radial values of velocity and acceleration are found to be:

$$\dot{R}(Z, t) = \dot{W}(t)\frac{\partial f(z)}{\partial z} = \dot{W}(t)f'(z) \tag{5a}$$

$$\ddot{R}(Z, t) = \ddot{W}(t)\frac{\partial f(z)}{\partial z} + \dot{W}^2(t)\frac{\partial^2 f(z)}{\partial z^2} = \ddot{W}(t)f'(z) + \dot{W}^2(t)f''(z). \tag{5b}$$

Substituting (5a) and (5b) into eqn (1), the interaction pressure for a general nose shape is:

$$p(z, t) = P_{st} + A\dot{W}^2(t) \cdot [f'(z)]^2 + B\ddot{W}(t)f(z)f'(z) + B\dot{W}^2(t)f(z)f''(z). \tag{6}$$

It is assumed that the projectile nose surface is smooth and there is no friction resistance. The local resistive force is perpendicular to the nose surface and the contribution of the disc to the resistive force acting on the nose is therefore:

$$\begin{aligned} dP_Z(z, t) = 2\pi p(z, t)f'(z)\,dz = 2\pi\{&f(z)f'(z)p_{st} + A\dot{W}^2(t)f(z)[f'(z)]^3 \\ &+ B\ddot{W}(t)f^2(z)[f'(z)]^2 + B\dot{W}^2(t)f^2(z)f'(z)f''(z)\}\,dz \end{aligned} \tag{7}$$

It is now assumed that full contact exists between the nose and the surrounding medium.

The total resistive force acting on the projectile at time t is therefore:

$$P_Z(t) = 2\pi \int_{z=0}^{z=L} M(f, f', f'')\,dz. \tag{8}$$

where:

$$\begin{aligned} M(f, f', f'') = &p_{st}f(z)f'(z) + A\dot{W}^2(t)f(z)[f'(z)]^3 + B\ddot{W}(t)f^2(z)[f'(z)]^2 \\ &+ B\dot{W}^2(t)f^2(z)f'(z)f''(z) \end{aligned} \tag{8a}$$

The optimal nose shape $f(z)$ is henceforward defined as that shape to which the minimum value of resistive force is developed. Minimization of the functional $P_Z(t)$ requires satisfying Euler's equation[12]:

$$\frac{dM(f, f', f'')}{df} - \frac{d}{dz}\frac{dM(f, f', f'')}{df'} + \frac{d^2}{dz^2}\frac{dM(f, f', f'')}{df''} = 0. \tag{9}$$

Operating expression (9) on eqn (8a) and using (1b, c) yields:

$$\rho_0\dot{W}^2(t)\{[f'(z)]^3 + 3f(z)f'(z)f''(z)\} + 2B\ddot{W}(t)\{f(z)[f'(z)]^2 + f(z)f''(z)\} = 0. \tag{10}$$

It will be benefited if eqn (10) is written in terms of the nondimensional parameters:

$$\xi = \frac{z}{L} \tag{11a}$$

$$f(z) = \frac{D}{2}\bar{f}(\xi) \tag{11b}$$

$$f'(z) = \frac{D/2}{L}\bar{f}'(\xi) \tag{11c}$$

$$f''(z) = \frac{D/2}{L^2}\bar{f}''(\xi). \tag{11d}$$

Hence:

$$-\bar{\alpha}\{[\bar{f}'(\xi)]^3 + 3\bar{f}(\xi)\bar{f}'(\xi)\bar{f}''(\xi)\} + \{\bar{f}(\xi)[f'(\xi)]^2 + \bar{f}^2(\xi)\bar{f}''(\xi)\} = 0 \tag{12}$$

where:

$$\bar{\alpha} = \frac{\rho_0\dot{W}^2(t)}{2BL\ddot{W}(t)} \quad \text{(nondimensional)}. \tag{13}$$

Equation (12) is a nonlinear second-order non-dimensional differential equation. The optimal non-dimensional nose shape function $\bar{f}(\xi)$ would satisfy eqn (12) and the boundary conditions:

$$\bar{f}(0) = 0; \tag{14a}$$

$$\bar{f}(1) = 1. \tag{14b}$$

A general solution is obtained as function of the nondimensional parameter $\bar{\alpha}$, i.e. for any depth to which certain velocity, acceleration and compressibility correspond, there is another optimal nose shape function.

SOLUTION PROCEDURE

Equation (10) can easily be solved for the two bounds of the problem:

Case I lower bound $\bar{\alpha} = 0$

In this case the equation becomes:

$$\bar{f}_0(\xi)[\bar{f}'_0(\xi)]^2 + \bar{f}^2_0(\xi)\bar{f}''_0(\xi) = 0 \tag{15}$$

where $\bar{f}_0(\xi)$ denotes the solution for the special case $\bar{\alpha} = 0$. Solution is straightforward and yields (Fig. 2 curve *F*):

$$\bar{f}_0(\xi) = \xi^{1/2}. \tag{16}$$

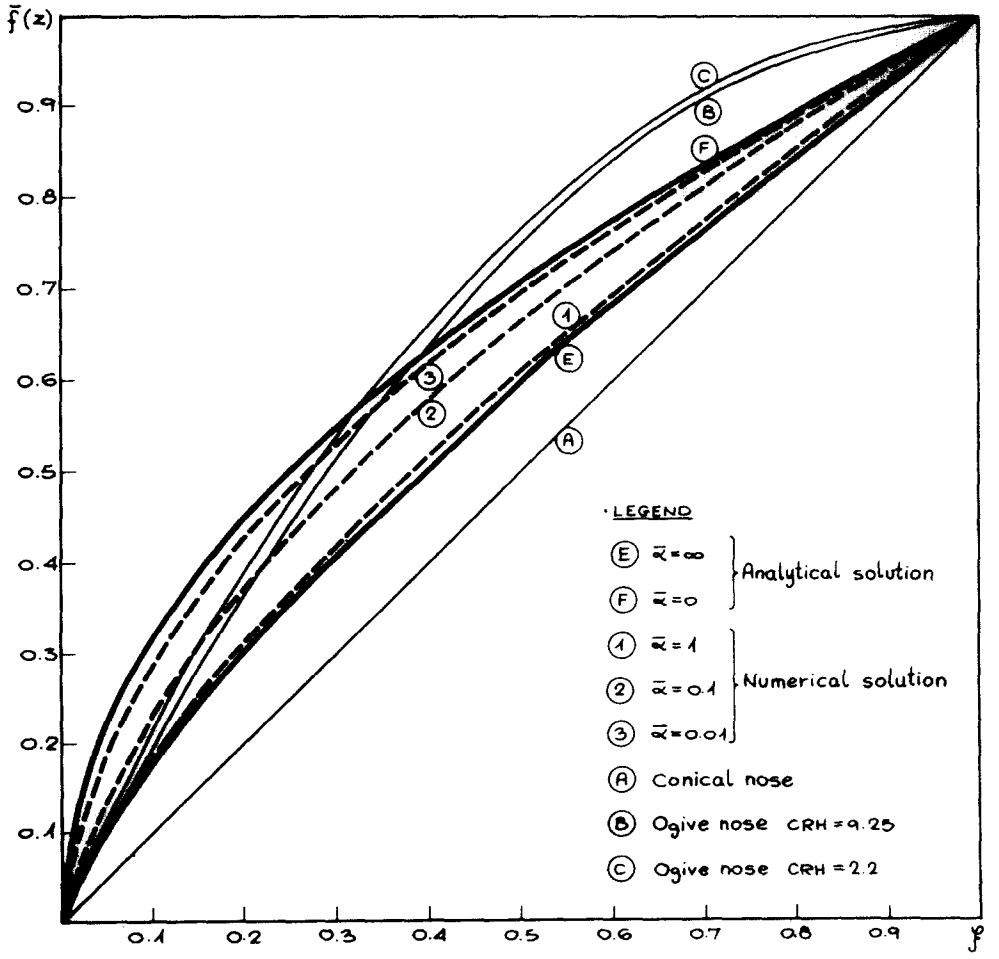

Fig. 2. Optimal nose shapes (non-dimensional).

Case II. Upper bound $\bar{\alpha} = \infty$

In this case eqn (13) reduces to:

$$[\bar{f}'_{\infty}(\xi)]^3 + 3\bar{f}_{\infty}(\xi)\bar{f}''_{\infty}(\xi) = 0 \tag{17}$$

of which the solution is:

$$\bar{f}_{\infty}(\xi) = \xi^{3/4}. \tag{18}$$

For all values of $\bar{\alpha}$: $0 < \bar{\alpha} < \infty$ a numerical scheme to solve eqn (13) has been adopted.

Divide the nose length L into N equal differences, the size of each is $\Delta = L/N$. Using central difference definitions transfers eqn (13) into the following nonlinear algebraic equation:

$$\begin{aligned}
&\bar{f}^3_{i+1}(\xi)\cdot\left[-\frac{\bar{\alpha}}{8\Delta^3}\right] + \bar{f}^2_{i+1}(\xi)\left[\frac{3\bar{\alpha}}{8\Delta^3}\bar{f}_{i-1}(\xi) - \frac{3\bar{\alpha}}{2\Delta^3}\bar{f}_i(\xi) + \frac{1}{4\Delta^2}f_i(\xi)\right] \\
&+ \bar{f}_{i+1}(\xi)\left[-\frac{3\bar{\alpha}}{8\Delta^3}\bar{f}^2_{i-1}(\xi) + \frac{3\bar{\alpha}}{\Delta^3}\bar{f}^2_i(\xi) - \frac{1}{2\Delta^2}\bar{f}_{i-1}(\xi)\bar{f}_i(\xi) + \frac{1}{\Delta^2}\bar{f}^2_i(\xi)\right] \\
&+ \left[\frac{\bar{\alpha}}{8\Delta^3}\bar{f}^3_{i-1}(\xi) - \frac{3\bar{\alpha}}{\Delta^3}\bar{f}^2_i(\xi)\,\bar{f}_{i-1}(\xi) + \frac{3\bar{\alpha}}{2\Delta^3}\bar{f}_i(\xi)\bar{f}^2_{i-1}(\xi) + \frac{1}{4\Delta^2}\bar{f}_i(\xi)\,\bar{f}^2_{i-1}(\xi)\right. \\
&\left. - \frac{2}{\Delta^2}\bar{f}^3_i(\xi) + \frac{1}{\Delta^2}\bar{f}_{i-1}(\xi)\,\bar{f}^2_i(\xi)\right] = 0.
\end{aligned} \tag{19}$$

There are $(N-2)$ equations, one for each internal point inside the boundaries, which, together with the boundary conditions (eqn 14a) determine the N unknowns. Solution starts at point $i = 2$ where $\bar{f}_{i-1}(\xi)$ is the boundary condition and $\bar{f}_i(\xi)$ is assumed. When the coefficients are known $\bar{f}_{i+1}(\xi)$ may be calculated. The coefficients for the next equation are then known, and the values of $\bar{f}_{i+1}(\xi)$ $(i = 3, \ldots, N)$ are calculated. If the calculated value $\bar{f}_N$ (ξ) deviates from the boundary conditions (14a), a corrected value for $\bar{f}_2(\xi)$ is assumed and a new set of $\bar{f}_i(\xi)$ is calculated.

$$\bar{f}_2(\xi)_{\text{assumed}} = \frac{\bar{f}_2(\xi)}{\bar{f}_N(\xi)}. \tag{20}$$

In all the studied cases convergence was achieved within $2 \div 3$ iteration.

NUMERICAL RESULTS AND CONCLUSIONS

Figure 2 shows some typical results and a few common nose shapes for reference. Curve A represents the family of noses having a conical shape, curves B and C represent the ogive noses CRH = 9.25 and CRH = 2.2 respectively. (An ogive nose has a circular shape which is defined by the parameter CRH, that is the ratio between the arc's radius and the projectile diameter.)

Analytical solution of eqn (13) shows the lower bound (curve F, eqn 16), and the upper bound (curve E, eqn 18). Curves 1–3 show numerical results for $\bar{\alpha} = 1$; 0.1; 0.01 correspondingly. For smaller values of $\bar{\alpha}$, curves approach the lower bound (curve F), and for $\bar{\alpha} > 1$ curves approach the upper bound (curve E). Though the solution is dependent on the parameter $\bar{\alpha}$ it may be seen that it is sensitive to the low range of $\bar{\alpha}$, namely $0.01 < \bar{\alpha} < 1$, and practically for $\bar{\alpha} > 1$ there exists a single optimal shape function independent of the instantaneous values of velocity and acceleration and of the volumetric strain.

The lower bound shape is much closer to the ogive nose shape rather than to the conical nose. It is in agreement with the experimental observation in the low velocity range that an ogive nose penetrates deeper than a conical nose of equal length and diameter[1].

In the special case where the penetrator is driven at a constant velocity, i.e. $\dot{W} = 0$, minimization of the reduced functional (8a) yields equation (17). Its solution is eqn (18), independent of the velocity. Taking that special case as an example, the total resistive force can be calculated when the nose shape is known. Calculating for the optimal nose at constant

penetration velocity yields:

$$_{\text{optimal}}P_Z(t) = \frac{\pi D^2}{4}\left\{p_{st} + [0.14063\,B + 0.10547\,\rho_0]\left(\frac{D}{L}\right)^2 \dot{W}^2(t)\right\}. \tag{21}$$

Where for a conical nose the resistance force is:

$$_{\text{conical}}P_Z(t) = \frac{\pi D^2}{4}\left\{p_{st} + [0.250\,B + 0.250\,\rho_0]\left(\frac{D}{L}\right)^2 \dot{W}^2(t)\right\}. \tag{22}$$

It should be noted that the resistive force in the discussed case of smooth surface decreases with slenderness and approaches the static term at an infinite slenderness. Fig. 3 shows the dependence of the dynamic term in eqn (21) on the volumetric strain and the nose slenderness. The resistive force on the optimal nose is very sensitive to the compressibility at the low range and only slightly affected by the compressibility for soft materials.

To conclude that example the normal interaction pressure distribution is calculated with aid of eqn (6), (18) and shown in Fig. 4. For the discussed case of penetration at constant velocity, a constant pressure acts on the conical nose, while it is variable on the optimal nose with higher pressure closer to the tip. Only along a limited length at the front which may vary between $15 \div 25\%$ of the nose length, there exist higher pressures on the optimal nose. At the tip, the tangent to the nose forms a right angle with the axis. The angle decreases repidly as is shown in Fig. 2. It has been found [9, 10] that the discs model predicts the projectile motion with

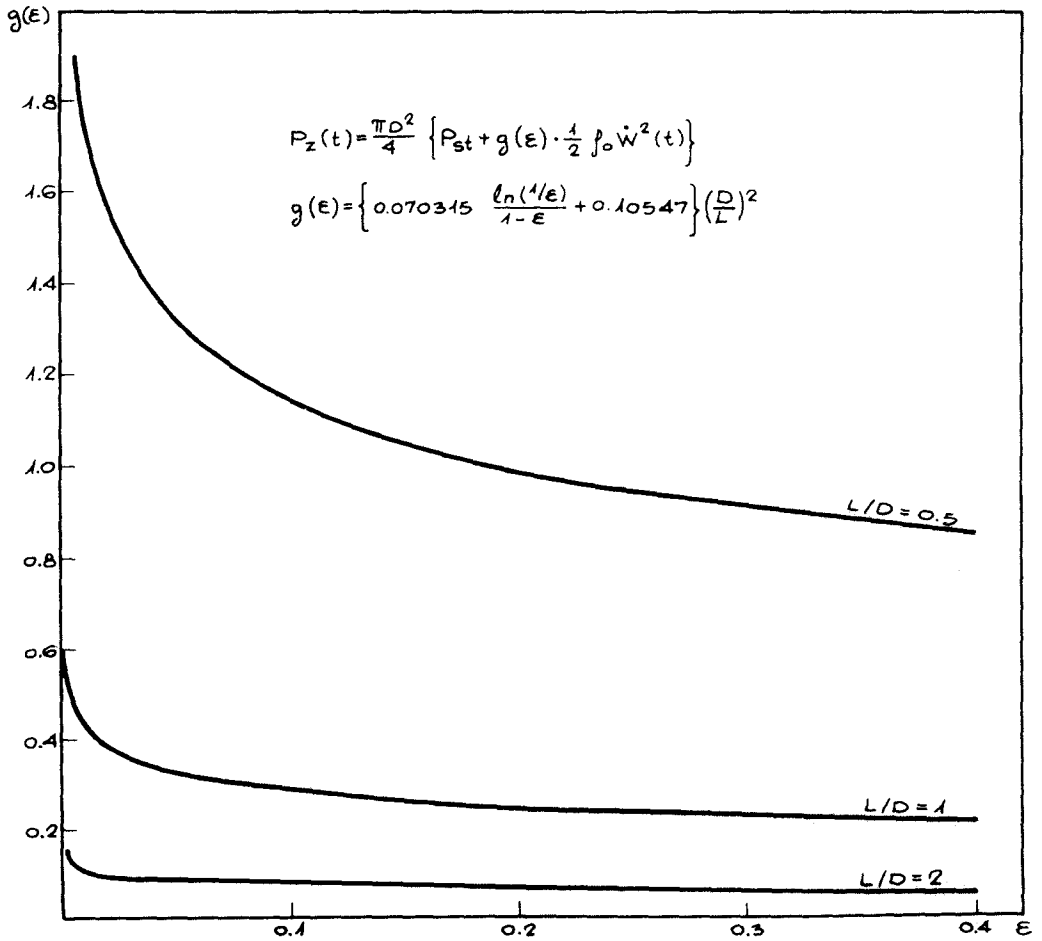

Fig. 3. Effect of compressibility on the dynamic resistive force.

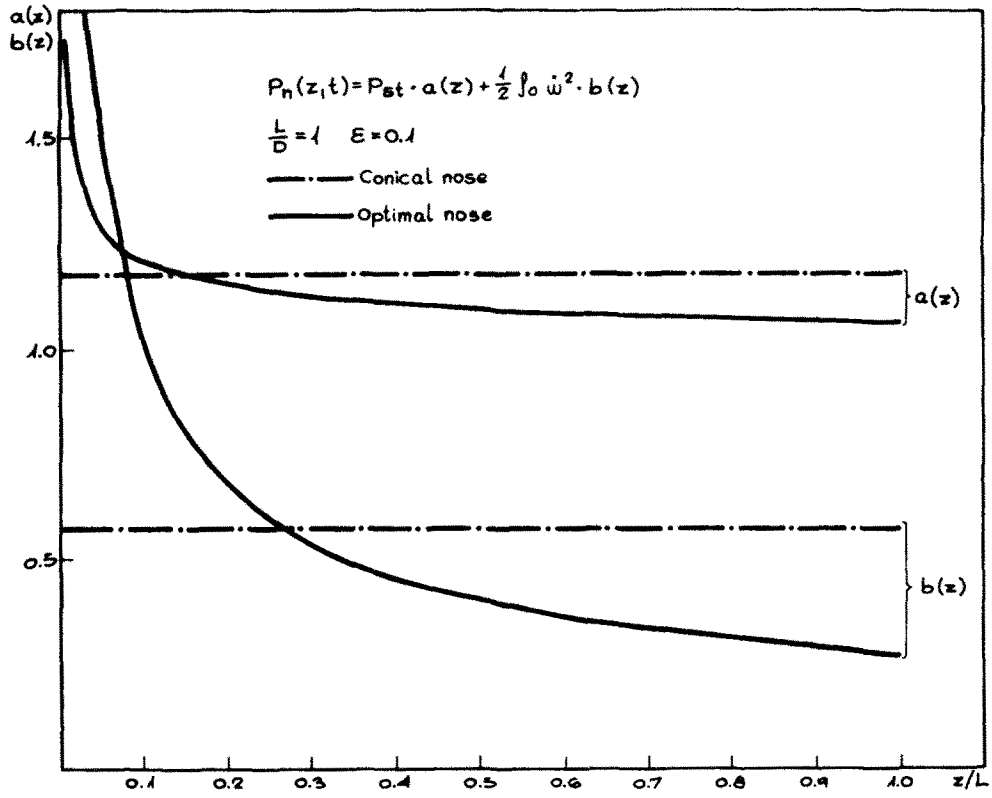

Fig. 4. Interaction pressure distribution.

very good correspondence with test data, however it is believed that the model represents better slender noses. It is believed therefore that the calculated stresses around the nose tip are less accurate relative to those at a certain distance from the nose tip.

REFERENCES

1. C.W. Young, Depth prediction for earth penetrating projectiles, *J. Soil Mech. Foundations Div. ASCE* **95**, 803–817 (1969).
2. C.W. Young, Empirical equations for predicting penetration performance in layered earth materials for complex penetrator configuration. Sandia Laboratories, Albuquerque, New Mexico, SC-RR-72-0523 (1972).
3. R.S. Bernard and S.V. Hanagud, Development of a projectile penetration theory. U.S. Army Waterways Experiment Station, Rep. S-75-9 (1975).
4. F.R. Norwood, Cylindrical cavity expansion in a locking soil. Sandia Laboratories, Alburquerque, New Mexico, SLA-74-0201 (1974).
5. P.F. Hadala, Evaluating of empirical and analytical procedures used for predicting the rigid body motion of an earth penetrator. U.S. Army Waterways Experiment Station, Rep. S-75-15 (1975).
6. L. Thigpen, Projectile penetration of elastic-plastic earth media. *J. Geotech. Div., ASCE* **100**, 279–293 (1974).
7. R.K. Byers and A.J. Chabai, Penetration calculations and measurements for a layered soil target. *Int. J. Num. Anal. Meth. Geomech.* **1**, 107–138 (1977).
8. M.H. Wagner, K.N. Kreyenhagen and W.S. Goerke, Numerical analysis of projectile impact and deep penetration into earth media. WES contract Rep. S-75-4, California Research and Technology Inc. (1975).
9. D.Z. Yankelevsky and M.A. Adin, A simplified analytical method for soil penetration analysis. *Int. J. Numer. Anal. Meth. in Geomech.* **4**, 233–254 (1980).
10. D.Z. Yankelevsky and J. Gluck, Nose shape effect on high velocity soil penetration. *Int. J. Mech. Sci.* **22**, 297–313 (1980).
11. L.E. Elsgolc, *Calculus of Variations.* Pergamon Press, Oxford (1962).